HMX CRYSTAL TOPOGRAPHY INVESTIGATED BY MEANS OF ATOMIC FORCE MICROSCOPY AND CONFOCAL MICROSCOPY

Michael Herrmann and Hubert Weyrauch

Fraunhofer Institut für Chemische Technologie ICT, D-76327 Pfinztal, Germany

E-Mail: michael.herrmann@ict.fraunhofer.de, hubert.weyrauch@ict.fraunhofer.de

ABSTRACT

The surface morphology of HMX grades (euhedral and subhedral) was investigated by means of atomic force microscopy and confocal microscopy. The crystals revealed quite different topographic structures, including step-shaped surfaces, outgrowths from the crystal bulk, fine particles intergrown to the bulk, surface roughness and in case of a type B grade HMX a highly defective surface layer. Stochastic methods were applied to quantify surface parameters such as the density and mean height of outgrowths/particles and the mean depth of the porous surface layer.

INTRODUCTION

The surface morphology of explosive particles influences important properties, such as abrasion, sensitivity and bonding behavior, e. g. when used in a plastic bonded explosive (PBX). For HMX a variety of commercial qualities are available on the market, reaching from standard variants to specially recrystallized RS-products (reduced sensitivity). The specifications of the products usually do not include surface or shape parameters, such as roughness, angularity or surface porosity. Therefore an approach was done to identify and quantify topographic parameters of HMX crystals, in order to compare and evaluate particle qualities and the influence of processing tools in future.

EXPERIMENTAL

Two qualities of coarse HMX crystals were investigated, including a rather euhedral habit[1] and in contrast a subhedral “type B” (grade B) quality from Dyno with poor developed, defective faces. From each quality, few crystals were selected and crystal surfaces were cleaned with compressed nitrogen to remove loose fine particles. Figure 1 compares for instance selected euhedral crystals (top) to type B crystals (bottom) with magnification factors 300 (top) and 500 (bottom).

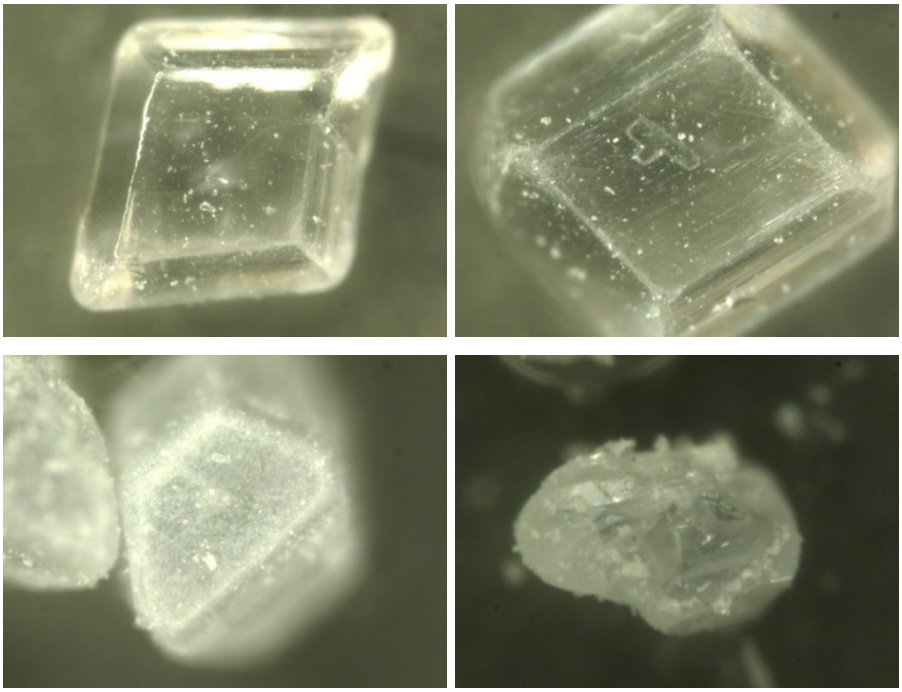

Figure 1 Microscopic pictures of the euhedral HMX (top) and type B HMX (bottom).

For characterization of the explosive crystals two 3D imaging systems were tested, a high-resolution atom force microscope AFM, Multimode, Controller V from Bruker and a confocal microscope µsurf custom from NanoFokus AG (Figure 2). With the AFM, surfaces were scanned with a cantilever tip using the TappingMode™, which enables imaging samples too fragile to withstand lateral forces. The technique maps topography by lightly tapping the surface with an oscillating probe with comparably high scan speeds. The cantilever’s

[1] Crystal habit is the characteristic external shape of an individual crystal or crystal group. A single crystal's habit is a description of its general shape and its crystallographic forms, plus how well developed each are. When the faces are well developed due to uncrowded growth a crystal is called euhedral, one with partially developed faces is subhedral, and one with undeveloped crystal faces is called anhedral (Wikipedia 2017).

oscillation amplitude changes with sample surface topography, and the topography image is obtained by monitoring these changes and closing the z feedback loop to minimize them. As cantilever a rotated monolithic silicon probe Tap300-G with 300 kHz resonant frequency, 40 N/m force constant and < 10 nm tip radius were used. The confocal microscope is equipped with a 505 nm LED light source and CCD camera. The system provides a contact-free surface metrology for topography and roughness measurements according to ISO standards with 0.3 µm horizontal resolution, even on surfaces with steep edges and areas with discontinuities.

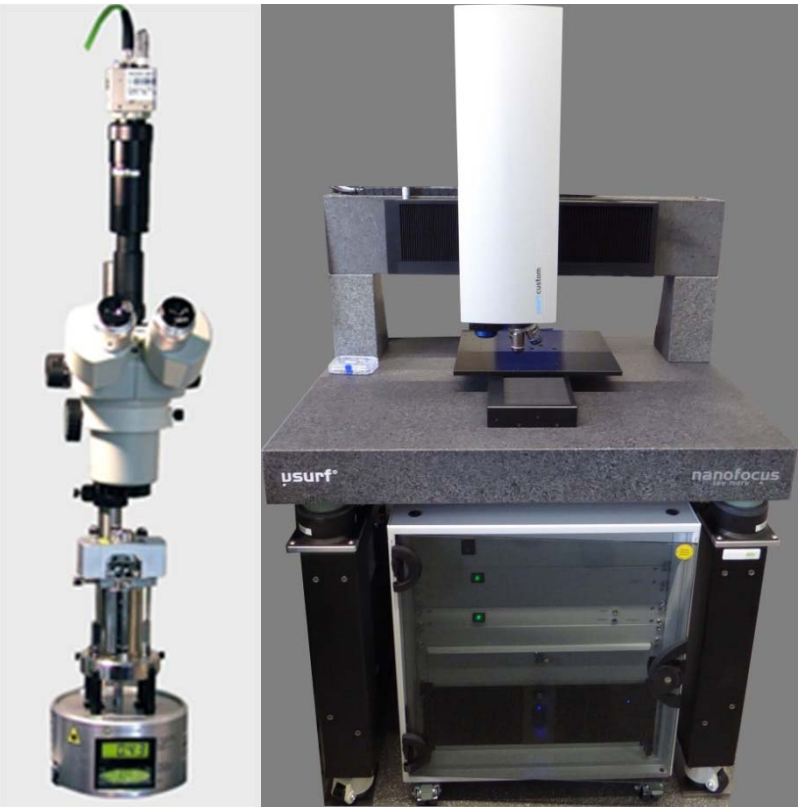

Figure 2 3D imaging systems applied to investigate the explosive crystal surfaces.

Comparative investigations of same surface sections on selected crystals were performed with both techniques. However, some systematic differences may arise due to the following items:

- It is hard to find exactly the same areas on the samples for the evaluation, technically,
- the methods provide different resolutions and
- different evaluation and positioning algorithms; e.g. evaluation of the roughness,
- piezo hysteresis occurs with the AFM, and
- the systems show (different) artefacts, particularly the AFM.

RESULTS

Euhedral crystals

Figure 3 depicts a euhedral crystal in the AFM with cantilever (left) and the same crystal captured with the confocal microscope (right). Even though the habit is well developed, the exposed face (010) shows plenty of defects and a steps structure. A prominent position is a T-shaped structure in the center of the crystal face, most likely due to an intergrowth of twins. Sections of 80 µm by 80 µm and 160 µm by 160 µm were scanned around the “T” with the AFM and the confocal microscope, respectively. The (3D) surface profiles of the scans are depicted in Figure 4.

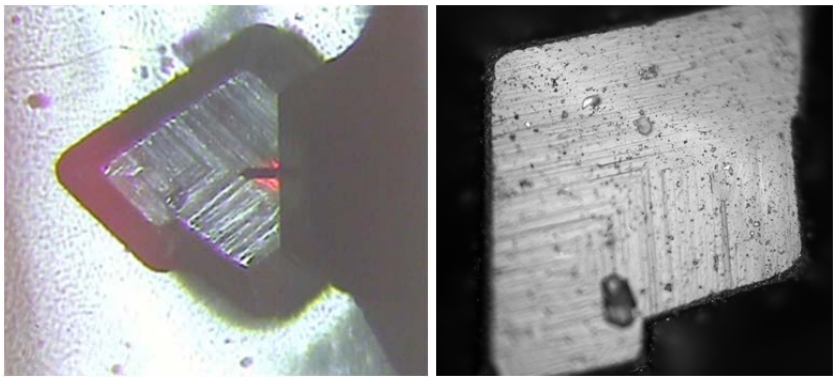

Figure 3 HMX crystal with cantilever in the AFM (left) and in the confocal microscope (right).

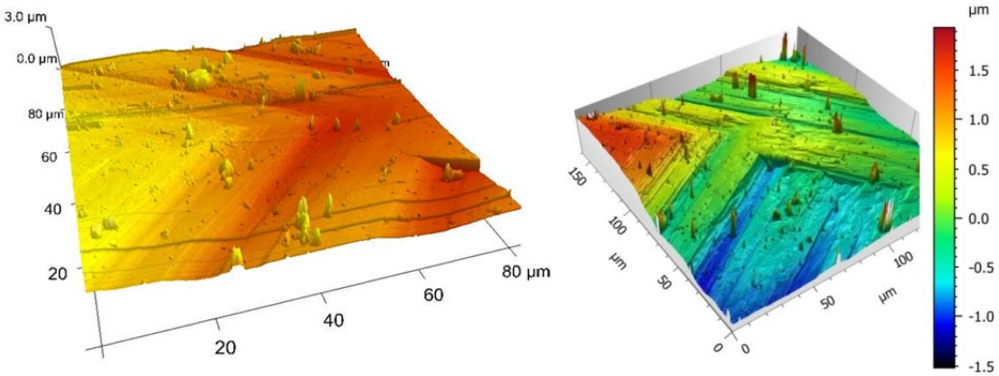

Figure 4 Surface profiles of selected areas (AFM left, CM right).

Both methods provided good topographic surface profiles and revealed step structures, local intergrown particles or outgrown structures, and a significant overlaying surface roughness, particularly in the image captured with the confocal microscope. In order to quantify the dimensions of surface structures selected cross sections were evaluated. For instance, in case of the surface sections depicted in Figure 4 two cutting lines were chosen; one bisecting the

angle of the left corner of the “T”, the other normal to the relatively deep edge near the right corner (Figure 5).

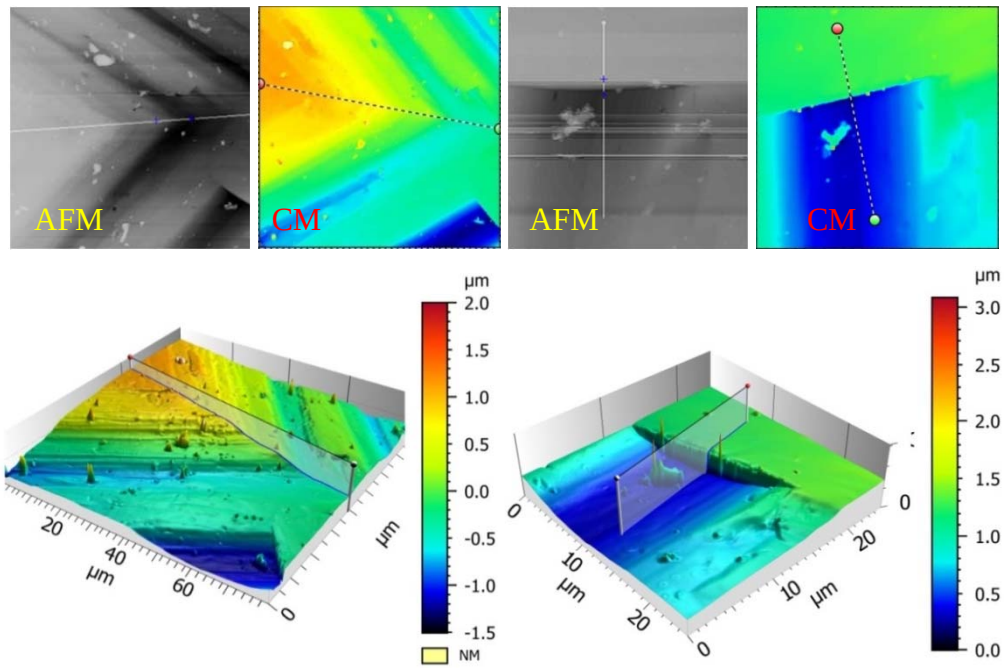

Figure 5 2D images captured with AFM (grey scaled) and CM (colored coded) and orientation/position of cutting lines (top) and related surface profiles captured with the confocal microscopy (bottom).

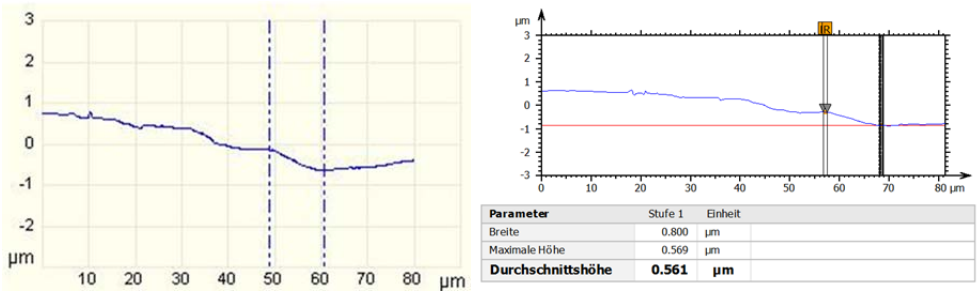

Figure 6 Height profiles of cross sections through the left T-corner (AFM left, CM right).

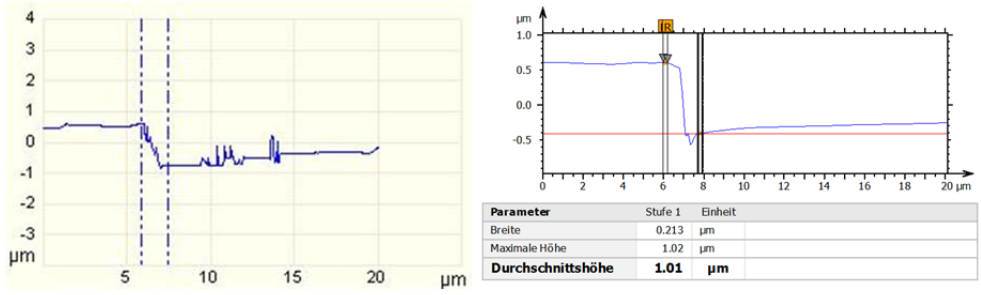

Figure 7 Height profiles of cross sections through the steep edge near the right T-corner (AFM left, CM right).

The height profiles of the cross sections are depicted in Figure 6 and Figure 7 for the left T-corner and the edge near the right T-corner, respectively. Both methods carved the step

structure clearly out, but some linear artefacts, visible as horizontal stripes in the top, third left image in Figure 5, emerge in the AFM profile as ragged spikes between 10 and 15 µm (Figure 7, left diagram). The corresponding profile obtained with confocal microscopy is smoother (Figure 6, left diagram); the method seems to be less prone to such kind of artefacts. The evaluation of the height profiles yielded 0.49 and 0.56 µm step height and 1.33 and 1.01 µm height of the edge near the right T-corner with AFM and confocal microscopy, respectively. Similar evaluation of a "terrace" shown in Figure 8 yielded a height of 3.1 µm.

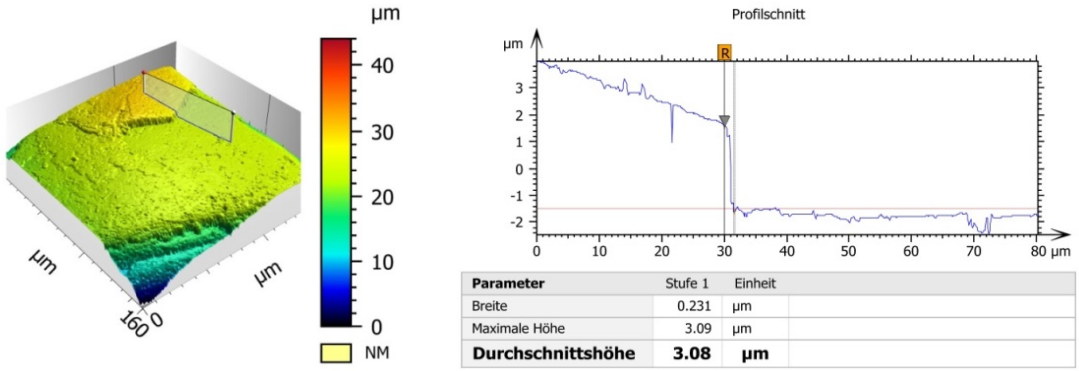

Figure 8 Crossing a terrace on a HMX crystal. 3D image (left) and height profile (right) observed with confocal microscopy.

In a further step the outgrowths or adhesive particles were investigated with the same techniques. The observed "spikes" are no artefacts, as they emerge in both methods. For instance in Figure 9 a cutting line was set to cross a spike and a church-shaped structure, and the evaluation yielded 0.79 µm height and 3.6 µm lengths of the "church nave". The "tower" of the church might have a height above 2.5 µm and a larger spike near the right corner of the images may reach even a height 6 to 7 µm. In this context it is noteworthy that the scaling of the height in the figure is by a factor >10 higher than those of the base, which results in a disproportionate height magnification. Besides, the confocal microscopy cannot monitor hidden parts of the structure, as depressions in a vertical wall or structures under overhangs, which would leave gaps in the displayed surface profiles. Therefore, gaps are closed in images with smoothed faces, calculated from neighboring data points, which may pretend bridging between particles/outgrowths and crystal bulk. Figure 10 shows xyz-normalized surface profiles including the church-shaped structure. Here gaps of "hidden surface parts" were left blank in the left picture and are complemented with flanks in the right picture. The figure gives evidence to at least partial bridging/intergrowth of the prominent structures to the crystal bulk, even for the large 7 µm particle. Besides, it shows some interesting details, such

as the circular elevation in the lower corner of the images or the cylinder-shaped tower of the “church”. Both seem to have their origin in internal defects in the bulk, e. g. in screw dislocations. And the connection of the “tower” via “nave” to the declining elevation between church and left corner of the images may also have its origin in a special internal defect structure of the crystal.

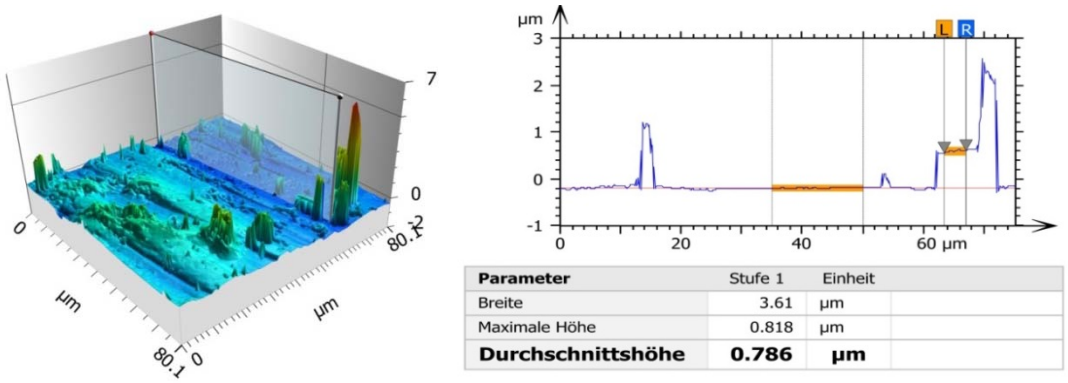

Parameter	Stufe 1	Einheit
Breite	3.61	µm
Maximale Höhe	0.818	µm
Durchschnittshöhe	**0.786**	**µm**

Figure 9 Surface profile with significant outgrowths/adhesive particles and marked cross section (left) and height profiles of the cross section, both obtained from confocal microscopy.

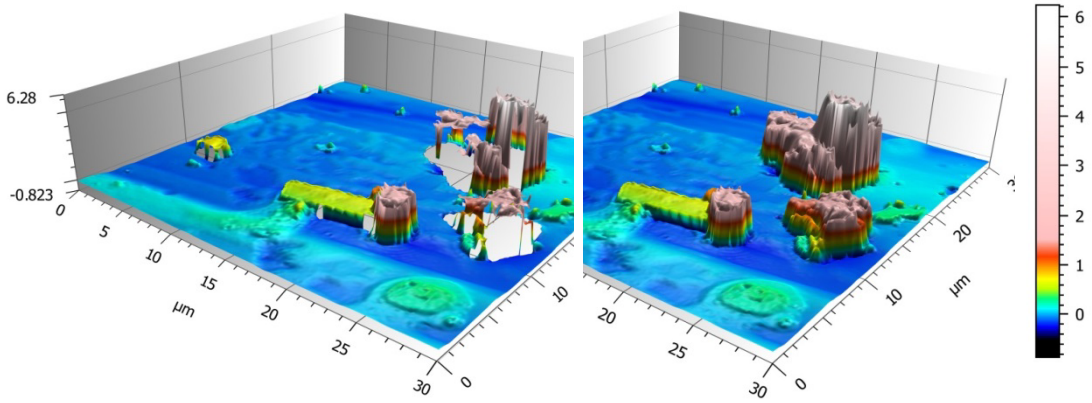

Figure 10 xyz-normalized presentation of a surface profile with blank “hidden parts” (left) and with closed faces (right).

Type B crystals

Figure 11 depicts the positioning of the AFM cantilever on a type B crystal face (left) and the same surface captured with the confocal microscope (right) and Figure 12 the resulting surface profiles. Obviously, the subhedral type B crystals exhibit a quit different surface morphology with still defined crystal habitus but rough surfaces and rounded edges and corners. The surface profiles revealed a highly uneven surface with depressions, protrusions, ditches, ridges and peaks. Accordingly, ragged height profiles were obtained from cross sections as shown in Figure 13, where for instance evaluation yielded recess depths of 0.8 µm.

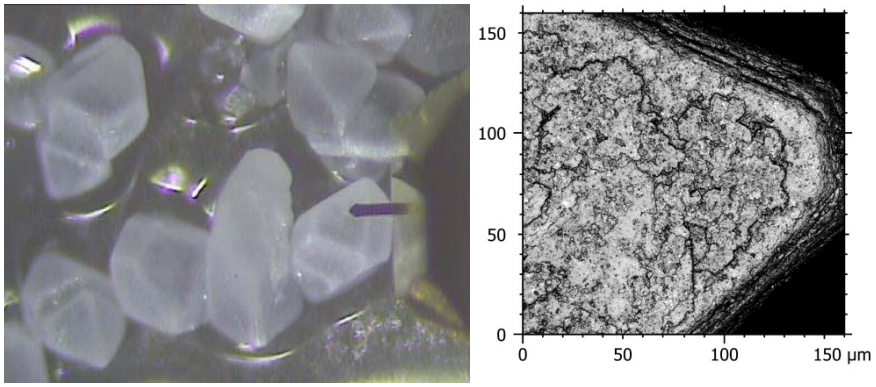

Figure 11 Cantilever of the AFM positioned on a type B crystal (left) and same surface captured with the CM-system (right).

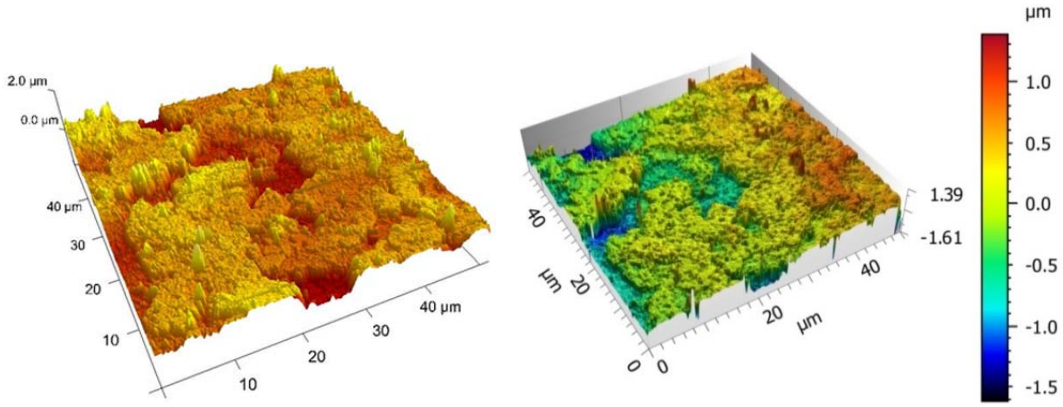

Figure 12 Surface profiles of type B crystal face. Identical section measured with AFM (left) and CM (right).

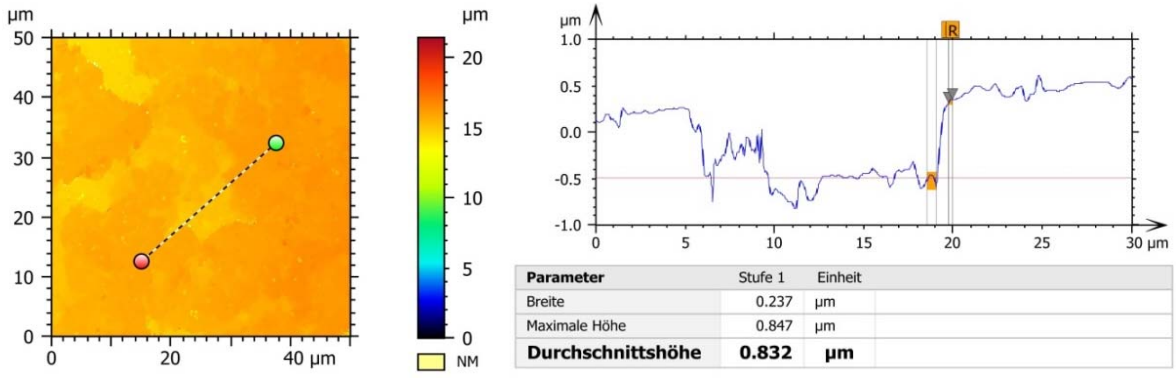

Figure 13 Cutting lines through recess on type B crystal face (left) and height profiles (right). Results obtained with confocal microscope.

Stochastic approaches to topographic parameters

So far the investigations provided a first view on surface morphologies of the HMX crystals and dimensions for a few selected structures. In order to obtain a representative quantification of surface properties, measurements of a variety of particles and surface sections combined with a statistical evaluation of structure parameters are required. In the following two

approaches to representative topographic parameters are described for quantification of the "spike" properties and of the porous, defective surface layer. In the first approach, a quantification of outgrowths/adhesive fine particles (spikes) on the otherwise relatively flat crystal surfaces of the euhedral HMX particles was tested. The method works best with flat almost horizontally oriented sections of crystal faces, where prominent HMX fragments can easily be distinguished from the crystal bulk. In order to provide a statistical basis six crystals (1, 3, 9, 12, 13, and 14 in Figure 14) and up to five surface sections per crystal were scanned with the confocal microscope, resulting in fifteen surface sections.

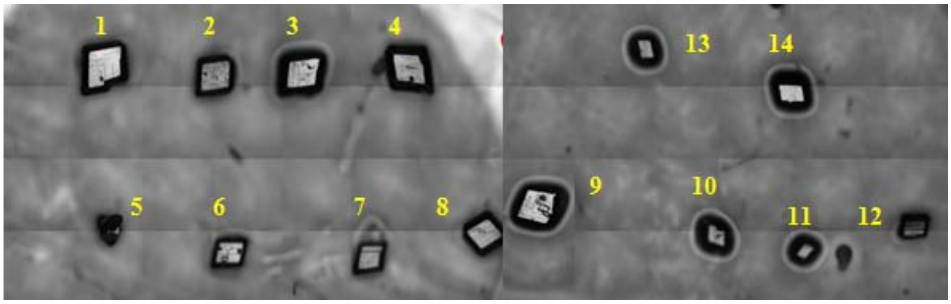

Figure 14 Crystal ensemble of euhedral HMX for testing quantification of outgrowths/adhesive particles.

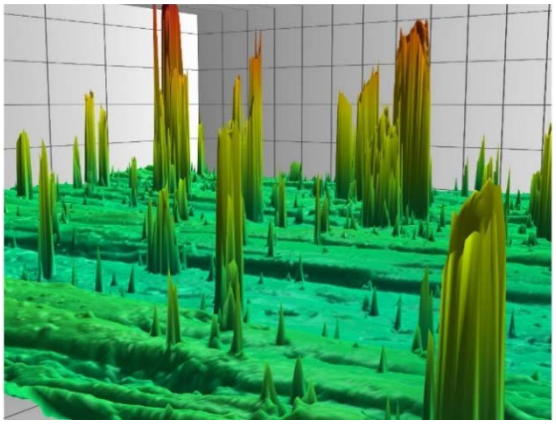

Figure 15 Topographic surface profile of crystal 1 with emphasized height magnification. Crystal face with a variety of outgrowths or intergrown particles apparent as spikes.

3D data sets were constructed by optical sectioning of the scans, smoothed by second-order polynomials providing flat reference planes, and hidden areas e. g. in steep sides were extrapolated for avoiding misinterpretations and counting errors. Figure 15 shows a surface profile (height map) of a selected section (of crystal 1) with an emphasized height magnification. For quantification of spike parameters surface fractions below distinct height thresholds of 0.3, 0.5, and 1 µm were cut, as depicted in Figure 16. Furthermore, the initial section size of 159 µm x 159 µm was reduced to 80 µm x 80 µm for the threshold at 0.3 and

0.5 µm in order to reduce interferences with the bulk, where e. g. smooth elevations or slightly tilted crystal faces may already reach the threshold heights within a larger section. As a further criterion spikes with areas below 0.2 µm^2 were excluded, in order to reduce effects of artefacts. For each spike the height and volume exceeding the threshold and the cross-section area at threshold height and for each surface section the spike densities, the relative cross-section (sum of spike cross-section areas divided by the base area), the corresponding relative volume and the mean and maximum spike heights were determined. The data were evaluated statistically revealing mean values, standard deviations, and standard errors calculated from the 15 surface sections (Table 1) with total numbers of 187 to 296 spikes at each threshold height.

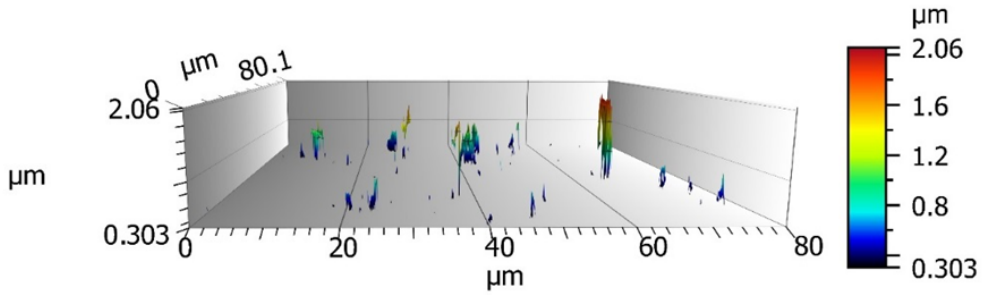

Figure 16 Topographic layer above 0.3 µm threshold height (80 µm x 80 µm base). For the evaluation data points below the threshold height were cut off.

Table 1 Results of the quantification of adhesive particles/outgrowths on crystal faces.

threshold [µm] area [µm^2]	0.3 6408	0.5 6408	1.0 25281
parameters	mean(std. error*) and (std. deviation)		
spike densities of sections [µm^{-2}]	0.00308(22) (0.00084)	0.00195(22) (0.00082)	0.00070(10) (0.0004)
spec. cross-section of sections [%]	0.73(14) (0.53)	0.37(8) (0.29)	0.90(24) (0.95)
spec. vol. of sections [µm]	0.0034(10) (0.0039)	0.0022(8) (0.0032)	0.0139(58) (0.022)
mean height of sections [µm]	0.55(4) (0.16)	0.53(4) (0.14)	0.71(7) (0.28)
max. height of sections [µm]	1.44(16) (0.61)	1.24(16) (0.62)	2.48(52) (2.01)
max. height [µm]	1.75	1.55	8.08/5.02/3.98

* standard errors in terms of the last digit

The mean spike densities decreased as expected with increasing threshold height from 3080 via 1950 to 700 mm^{-2} (Figure 17, left) and the standard errors between 100 and 220 mm^{-2} (7.1

to 14.3%) indicate significance of the results obtained with the 15 surface sections. The comparably high standard deviations between 2200 and 3900 mm^{-2} (27 to 57%) show that measurements of a single section only would not provide representative results – also expected. Beside the spike density, the mean and maximum spike heights of the sections are significant parameters. The mean heights range from 0.5 to 0.71 µm (relative standard errors between 7 and 10%) and the maximum heights from 1.74 µm (1.44 + 0.3) to 3.48 µm (2.48 + 1). The maximum heights of all outgrowths/adhesive particles reach values up to 4 to 8 µm.

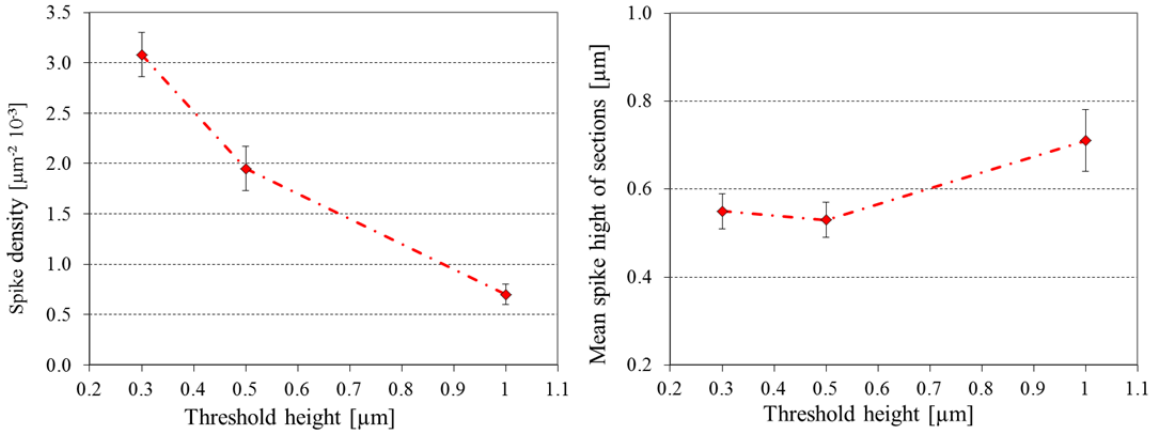

Figure 17 Spike densities (left) and mean spike heights (right) determined at 0.3, 0.5 and 1 µm threshold height and standard error bars.

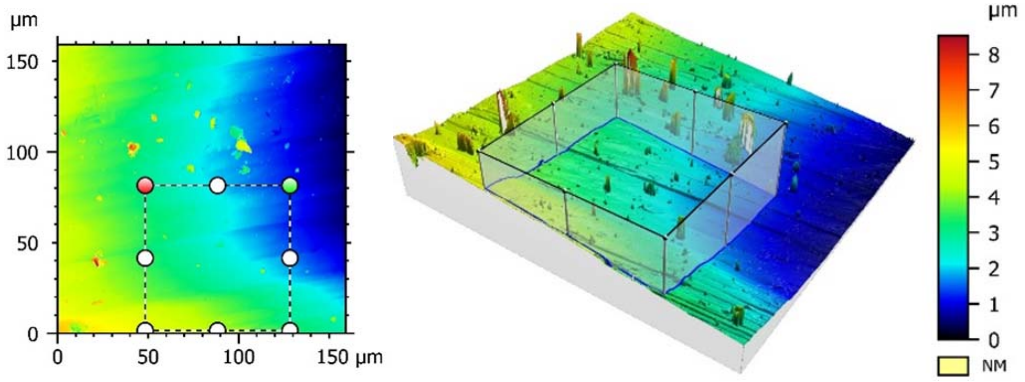

Figure 18 Positioning of an 80 µm x 80 µm section in the 159 x 159 $µm^2$ section. The smaller section excluded all large spikes and led to systematically reduced mean spike heights at 0.3 and 0.5 µm threshold height in Figure 17.

It is interesting to note that the mean heights of spikes exceeding the 1 µm threshold are larger than those exceeding 0.3 and 0.5 µm in Figure 17. The selection of the surface sections for the evaluation with the smaller threshold heights may explain this effect. For instance, Figure 18 depicts the positioning of an 80 x 80 $µm^2$ in the 159 x 159 $µm^2$ surface section. Obviously the large spikes are not captured with this positioning, resulting in a comparably smaller mean

spike height of the smaller section. In this case parameters obtained from larger section may be more representative than those from the subsection, and an improved selection of “representative” subsections shall be applied in future. The specific cross-sections and volumes of outgrowths/adhesive particles also may be used for a more detailed characterization, but these parameters seem to be prone to deviations and systematic errors.

Height profiles of five type B crystals were measured with the confocal microscope in the second approach, and were evaluated with the aim of determining the depth of the defective (porous) surface layer. For instance Figure 19 depicts a 2D color coded image (left) of a selected crystal face with a cutting line near the left lower corner of the image and related the height profile (right). The two marked sections in the profile present the bottom and the upper rim of the defective layer and its height difference the local depth of the defective surface layer, which yielded 0.64 and 0.58 µm maximum and medium height for the case depicted. The data obtained by this method are summarized in Table 2. In total 42 height profile sections were evaluated, yielding a mean depth of the defective layer of 1.58 ± 0.18 µm and maximum values as high as 4 to 6 µm. With about 11% standard error, the evaluation also provides a significant parameter for characterizing such kind of crystal surface morphology.

Table 2 Results of the quantification of defective layer depth of the subhedral type B crystals.

Crystal #	cross-sct. #	c-s length [µm]	depth [µm]		cross-sect. #	c-s length [µm]	depth [µm]
crystal 7	1	62	1.11	crystal 13	1	22.6	0.94
			1.38		2	45.4	2.08
	2	28.9	0.87				1.94
			0.96				1.14
	3	28	1.58				2.72
	4	23.4	1		3	20	2.02
			1.74		4	28.6	1.32
	5	33.9	0.92				0.81
			1.83		5	22.4	1.15
crystal 8	1	35.3	0.81				2.2
	2	15.7	0.78	crystal 16	1	127	1.76
	3	118	1.8				2.1
			1.00		2	112	1.51
	4	69.9	0.55				3.7
	5	25.1	1.2		3	38.6	4.29
crystal 11	1	51.8	0.64		4	46.4	5.94
	2	87.2	0.42				1.59
	3	49.3	0.50		5	56.6	1.7
	4	81.4	0.70				3.91
			0.81				
	5	102	1.12			mean	1.58
			0.42			std. error	0.18

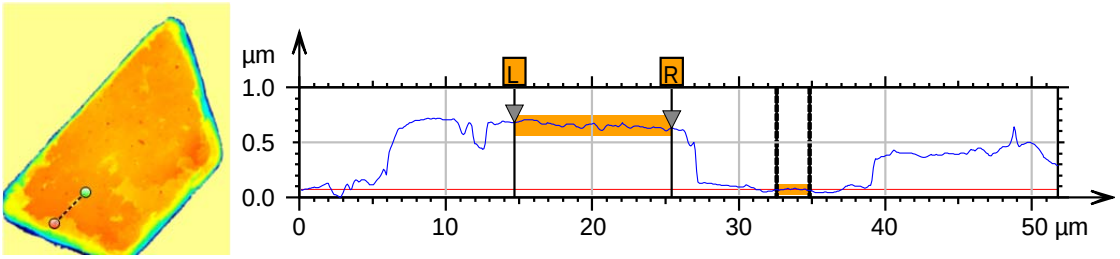

Figure 19 Positioning of a cutting line on crystal 11 (left) and 2D height profile by the line (right). The evaluation yielded a depth of the defective surface layer 0.64 µm (evaluated section are marked in orange).

SUMMARY

Both methods, the atomic force microscopy and the confocal microscopy, provided valuable information and well resolved surface profiles of crystals faces, but the confocal microscopy turned out as more easily applicable for this work and less prone to artefacts. The investigated HMX crystal grades exhibited highly differing surface characteristics. Closed step-shaped surfaces with a slight overlaying surface roughness were found on the “euhedral” crystals. Besides, a variety of fine adhesive, intergrown particles and small outgrowths were detected on crystal faces, the latter most likely originated from internal crystal defects. Highly defective crystal faces were found on the type B “subhedral” crystals with a rather porous highly ragged surface layer, depressions, protrusions and ridges. The features were quantified with stochastic methods, which provided significant topographic parameters, e. g. the density and mean height of outgrowths/particles and the mean depth of the porous surface layer. The dimensions of the structures range from 0.5 µm (step height) to about 3 µm (particle/outgrowth) heights, but singularly up to 7 µm, and 1.6 µm mean depth height of the porous layer of the type B crystals, but maximum values up 6 µm.

The topographic features observed are considered to influence the properties of HMX crystals in explosive applications. For instance, spikes may initiate hot spots, when particles are pressed one against another through mechanical loading, and surface micro-pores on particle surface are discussed to increase the sensitivity through pore collapse[2]. On the other hand, porosity and surface roughness influence mechanical aspects such as the stability against abrasion and the wetting and bonding behavior in composites, e.g. plastic bonded explosives.

---

[2] Springer, H. K., S. et al. (2018), Modeling The Effects of Shock Pressure and Pore Morphology on Hot Spot Mechanisms in HMX, *Propellants, Explosives, Pyrotechnics* **43**(8), 805-817

Here a moderate roughness may mediate wetting and adhesive properties. Highly uneven surfaces with small but deep ditches may hinder a proper wetting leaving unfilled voids/pores or poorly connected interfaces between crystal and binder, but very flat surfaces reduce the specific interface area and thus adhesion energy, and besides may influence the wetting behavior (lotus effect).

The investigations yielded results of two crystal grades and quantification of a few selected parameters/topographic features. Further investigations shall broaden the view and include further morphologic parameters, such as the surface roughness and the dimension and densities of open surface pores, and should include further HMX grades or even further explosives. And of course, the parameters have to be correlated with the macroscopic properties of the crystals, when used in a PBX.

ABBREVIATIONS

AFM	Atomic force microscope
CM	Confocal microscope
HMX	Cyclotetramethylene tetranitramine, high explosive
ICT	Fraunhofer Institut für Chemische Technologie, Pfinztal, Germany
PBX	Plastic bonded explosive
RDX	Cyclotrimethylene trinitramine, high explosive
RS	Reduced Sensitivity (quality feature of explosives, e.g. RS-HMX)